Biocompatible and thermo-responsive nanocapsules through vesicle templating

Polymer Chemistry

PAPER

View Article Online
View Journal | View Issue

Cite this: *Polym. Chem.*, 2014, **5**, 4569

Biocompatible and thermo-responsive nanocapsule synthesis through vesicle templating†

Garbiñe Aguirre,[a] Jose Ramos,[a] Johan P. A. Heuts[b] and Jacqueline Forcada*[a]

Received 27th February 2014
Accepted 7th April 2014

DOI: 10.1039/c4py00297k

www.rsc.org/polymers

Thermo-responsive and biocompatible cross-linked nanocapsules were synthesized through dimethyldioctadecylammonium bromide (DODAB) vesicle templating. For this, firstly two random copolymers, *N*-vinylcaprolactam (VCL) and acrylic acid (AA), with different chain lengths but using the same monomer ratio, were synthesized by reversible addition–fragmentation chain transfer (RAFT) polymerization. These anionic random copolymers were adsorbed onto cationic DODAB vesicles. Then, biocompatible and thermo-responsive nanocapsules were obtained by semicontinuous emulsion polymerization under monomer-starved conditions for both the main monomer (VCL) and the cross-linker. Although in all the cases the typical thermal behavior of PVCL-based nanocapsules was observed, hysteresis between cooling and heating cycles was observed at low temperature in the case of non-cross-linked nanocapsules. This behavior was reduced using different types and amounts of cross-linkers. In addition, transmission electron microscopy (TEM) characterization demonstrated the successful formation of nanocapsules either with short or long random copolymers. The formation of stable nanocapsules was confirmed below and above the volume phase transition temperature (VPTT) by surfactant lysis experiments through optical density and DLS measurements in all the nanocapsules synthesized. These biocompatible and thermo-responsive nanocapsules could be suitable and potentially useful as nanocarriers for drug delivery.

1. Introduction

The use of nanotechnology in medicine and more specifically in drug delivery is set to spread rapidly. Since many drug potencies and therapeutic effects are limited or otherwise reduced because of the partial degradation that occurs before they reach the desired target in the body, the design of a suitable carrier is necessary.[1] Among them, polymeric responsive nanocapsules are of particular interest because of their special hollow morphology and potential for the encapsulation of a variety of guest substances within their empty core domain.[2–4]

To make the load and release of substances from the resultant hollow spheres controllable, it is desirable to develop further so called "smart" nanocapsules, which can switch their structure reversibly from a closed to an open state with the help of external stimuli such as temperature, pH, pressure, ionic strength, magnetic field, light, ultrasound and enzymes among others.[5–8] Special attention is paid to nanocapsules based on temperature-sensitive polymers, which have a lower critical solution temperature (LCST) near the physiological one, because of their potential use as controlled drug delivery systems. Although in most of the published reports, poly(*N*-isopropylacrylamide) (PNIPAM) has been used as a thermo-responsive polymer,[9–11] the use of poly(*N*-vinylcaprolactam) (PVCL) is a better alternative due to its biocompatibility.[12,13] In comparison with PNIPAM, the amide group of PVCL is directly connected to the hydrophobic carbon–carbon backbone chain and therefore, its hydrolysis will not produce small amide compounds, which are unwanted for biomedical applications.[14]

To date, various routes leading to hollow particle morphologies have been explored. However, the application of hollow micro or nanocapsules could be limited mainly because of the disadvantages associated with the techniques used for their synthesis. The harsh conditions employed in some methods make them unsuitable for the encapsulation of sensitive materials due to their polydispersity and uneven shell coverage. Many groups have used amphiphilic block copolymers to form core–shell micelles and vesicles by a self-assembly method.[15–17] Despite the approach being successful in forming nanocapsules, it was unable to control their inner diameters.

An alternative route for the synthesis of nanocapsules is colloidal templating as in the case of the layer-by-layer method. This method involves consecutive deposition of oppositely charged polyelectrolytes, mainly by electrostatic attraction, from dilute solutions onto a colloidal substrate.[18–20] Despite its

[a]*POLYMAT, Bionanoparticles Group, Departamento de Química Aplicada, UFI 11/56, Facultad de Ciencias Químicas, Universidad del País Vasco UPV/EHU, Apdo. 1072, 20080 Donostia-San Sebastián, Spain. E-mail: Jacqueline.forcada@ehu.es*

[b]*Laboratory of Polymer Materials, Eindhoven University of Technology, PO Box 512, 5600 MB Eindhoven, The Netherlands*

† Electronic supplementary information (ESI) available. See DOI: 10.1039/c4py00297k

simplicity, several polyelectrolyte layers must be deposited, the cross-linking of them often being needed, in order to obtain more stable structures.[21,22] Furthermore, in order to obtain a hollow structure it is necessary to remove the template and this can provoke the disruption of the nanocapsule. Therefore, nowadays the use of soft templates, such as emulsion droplets, biological cells, and surfactant vesicles is gaining interest. Among them, vesicles, which are closed bilayer aggregates formed from phospholipids and surfactants, are very useful due to their easy preparation with controllable sizes. On the one hand, vesicles are able to internalize hydrophobic monomers into their surfactant bilayer and therefore, subsequent polymerization could lead to the formation of hollow nanocapsules.[23,24] On the other hand, vesicles have been explored successfully as soft templates in the layer-by-layer approach offering different advantages over conventional substrates. Among them, there is the possibility of pre-encapsulation of different substances before the formation of the nanocapsules.[25,26]

With the aim of avoiding the necessity of deposition of several layers in order to obtain stable nanocapsules, van Herk and co-workers recently demonstrated the effectiveness of a simple RAFT-based vesicle templating approach for the synthesis of water filled non-cross-linked and cross-linked polymeric nanocapsules.[27,28] In the first case, Ali *et al.*[27] synthesized non-responsive nanocapsules and in the second case,[28] they synthesized pH-responsive cross-linked nanocapsules through the hydrolysis of the tertiary butyl ester groups of the shells. In both studies, firstly small polyelectrolytes, synthesized by the RAFT process, were adsorbed on vesicles and taking advantage of having living RAFT moieties on vesicles, robust nanocapsules were obtained through monomer addition at controlled rates. As a drawback, pH-responsive nanocapsules obtained by acid hydrolysis in dioxane required an exhaustive purification to transfer them to the aqueous phase.

In this work, the synthesis of biocompatible and thermo-responsive nanocapsules based on PVCL through vesicle templating is reported for the first time. For that, cationic vesicles of dimethyldioctadecyl ammonium bromide (DODAB) were prepared by an extrusion process. On the other hand, random copolymers with different lengths but the same ratio of *N*-vinylcaprolactam (VCL) and acrylic acid (AA) monomeric units were synthesized by RAFT polymerization using dibenzyl trithiocarbonate (DBTTC) as the RAFT agent. After carrying out the adsorption of the random copolymers onto DODAB vesicles, they were chain extended by semicontinuous emulsion polymerization under monomer-starved conditions for both the main monomer (VCL) and the cross-linker in order to obtain a polymer shell around the vesicles, and in this way, producing biocompatible and thermo-responsive nanocapsules. Colloidal characteristics, such as the changes in the average hydrodynamic particle diameter and swelling ratio at different temperatures, were measured by Photon Correlation Spectroscopy (PCS). Transmission electron microscopy (TEM) was used for the direct observation of the new biocompatible and thermo-responsive nanocapsules. In addition, in order to assess the stability of the synthesized nanocapsules, surfactant lysis experiments were carried out.

2. Experimental section

2.1 Materials

Dimethyldioctadecyl ammonium bromide (DODAB, Acros), *N*-vinylcaprolactam (VCL, Sigma-Aldrich), acrylic acid (AA, Fluka), *N*,*N*′-methylenebisacrylamide (MBA, Sigma-Aldrich), ethylene glycol dimethacrylate (EGDMA, Sigma-Aldrich), and Triton X-100 (TX-100, Sigma-Aldrich) were used as supplied. The RAFT agent dibenzyl trithiocarbonate (DBTTC) was synthesized as described in a previous work.[29] Initiator *N*,*N*′-azobis(isobutyronitrile) (AIBN, Fluka) was re-crystallized from methanol and the water-soluble azo initiator 4,4′-azobis 4-cyanovaleric acid (V-501, Fluka) was used as received. Dioxane (Merck) and dimethyl sulfoxide-d_6 (Campro scientific) were all used without any treatment. Double deionized (DDI) water was used throughout the work.

2.2 Vesicle preparation

Large unilamellar vesicles (LUVs) were prepared by a membrane extrusion method following the procedure described previously by Ali *et al.*[27] Briefly, 10 mM DODAB dispersion was passed through a 200 nm polycarbonate filter at 60 °C five times. After extrusion, the vesicle dispersion was kept overnight at 60 °C. The average diameter measured by dynamic light scattering (DLS) was found to be around 160 nm (PDI = 0.131) and the gel-to-liquid crystalline phase transition temperature (T_m), determined spectrophotometrically, was 37.5 °C.

2.3 Synthesis of anionic random RAFT copolymers

Two random RAFT copolymers with different chain lengths but the same ratio between VCL and AA monomeric units (VCL_9-*co*-AA_6 and VCL_{18}-*co*-AA_{12}) were synthesized in dioxane using dibenzyl trithiocarbonate (DBTTC) as the chain transfer agent. They were synthesized as follows: 21 mM of VCL, 14.4 mM of AA and 0.5 mM of DBTTC (in the case of VCL_9-*co*-AA_6) or 0.25 mM of DBTTC (to obtain VCL_{18}-*co*-AA_{12}) were mixed in 26 mL of dioxane in a three-neck Schlenk flask. The mixture was purged with argon for 1 h before starting the copolymerization reaction. After adding the initiator (AIBN), maintaining [DBTTC]/[AIBN] = 10, the copolymerization reaction was allowed to continue under stirring and an argon atmosphere at 70 °C up to 20% of partial conversions of VCL and AA. The random copolymers synthesized were dialyzed against distilled water and then the water was evaporated with a rotary evaporator.

2.4 Adsorption studies

Calculated amounts of RAFT copolymer were transferred in different vials from a 10 mM aqueous stock solution of RAFT copolymer. Then, equal volumes of vesicle dispersion (10 mM) were added dropwise into these vials under stirring. The pH of all the dispersions was around 7. Particle size measurements were performed on these samples. The normalized hydrodynamic diameter was calculated following the expression: d/d_o, in which d is the average hydrodynamic diameter at any mixture composition at 55 °C and d_o is the average hydrodynamic diameter of the naked vesicles at 55 °C.

2.5 Synthesis of nanocapsules

Thermo-sensitive nanocapsules were synthesized by semi-continuous emulsion polymerization under monomer-starved conditions for both the main monomer (VCL) and the cross-linker (MBA or EGDMA) in a 25 mL three-neck Schlenk flask equipped with a magnetic stirrer bar and a heating bath. A calculated amount of RAFT copolymer (from a 10 mM stock solution of RAFT copolymer) was transferred into the flask and then a calculated amount of vesicle dispersion (10 mM) was added dropwise under constant stirring at 70 °C. The flask mixture was purged with argon for 30 min. After adding the water-soluble initiator (the ratio of RAFT agent to initiator concentrations was maintained 2 : 1), 0.1 g (0.72 mmol) of VCL and a variable amount (from 4 to 12 mol% with respect to VCL) of cross-linker (EGDMA or MBA) were fed at a rate of 0.005 g min^{-1} using a Dosimat autotitrator. After the completion of both the main monomer (VCL) and cross-linker (MBA or EGDMA) feeding, the reactor was kept stirring at 70 °C for another 2 h.

2.6 Surfactant lysis experiments

2 mL of nanocapsule dispersion (1 mM) was added to a screw-capped quartz cuvette (1 cm optical path length), then it was heated and equilibrated at 50 °C. 20 μL aliquots of 200 mM Triton X-100 solution were injected repeatedly into the sample while stirring inside the cuvette. The optical density (as absorbance at 450 nm) was recorded at 2 min after every injection. Furthermore, the optical density was recorded after equilibrating the sample at 20 °C in order to probe the stability at low temperature.

2.7 Characterization

Characterization of the RAFT copolymers. The evolution of the partial conversion of VCL and AA during copolymerization was determined by quantitative proton nuclear magnetic resonance spectroscopy (^{1}H-NMR) using dimethyl formamide (DMF) as the internal standard and dimethyl sulfoxide-d_6 as the solvent. Prior to the analysis of the samples by NMR, a calibration curve of each monomer (VCL and AA) was made. The molecular weight of the random copolymers was measured by ^{1}H-NMR end group analysis. ^{1}H-NMR spectra were recorded by using a Varian 400 MHz spectroscope.

Colloidal characterization of the nanocapsules. Colloidal characteristics of the nanocapsules synthesized, such as the average hydrodynamic diameters at different temperatures, were measured by photon correlation spectroscopy (PCS, Zetasizer Nano ZS instrument, Malvern Instruments). The sample was directly taken from the reactor and measurements were carried out from 60 to 10 °C taking measurements every 2 °C with 10 min being the stabilizing time between measurements. The swelling ratio was calculated following the expression: $(dp_T/dp_{60})^3$, in which dp_T is the average hydrodynamic diameter at any temperature and dp_{60} is the average hydrodynamic diameter at 60 °C.

Transmission Electron Microscopy (TEM, TECNAI G^2 20 TWIN 200kV LaB_6) was used for the direct observation of the nanocapsules. A diluted sample (0.07 wt%) drop was placed on a carbon film copper grid, which has previously been hydrophilized by a glow discharge process. Then, the sample was rotated at 2000 rpm in order to dry quickly at room temperature by a spinning process.

The gel-to-liquid crystalline phase transition temperature (T_m) of the vesicles and nanocapsules was determined spectrophotometrically using the dependence of the absorbance on temperature. Measurements were done using a Hewlett-Packard Photodiode Array UV spectrophotometer equipped with a Peltier heater-cooler. Samples were measured in a screw-capped quartz cuvette and recorded from 20 to 55 °C with 2.5 °C increments and a stabilizing time of 2 min between measurements.

3. Results and discussion

3.1 Synthesis and characterization of the anionic random RAFT copolymers

Random copolymers with different lengths but having the same ratio of *N*-vinylcaprolactam (VCL) and acrylic acid (AA) units were synthesized by means of reversible addition–fragmentation chain transfer (RAFT) polymerization in solution using dibenzyl trithiocarbonate (DBTTC) as the chain transfer agent. Random copolymers were chosen instead of block copolymers in order to minimize the formation of micelles. In this way, the formation of new particles by secondary nucleations could be minimized during the synthesis of polymeric nanocapsules by emulsion polymerization. Due to the different reactivity ratios of AA and VLC, the reactivity ratio of AA being much higher than that of VCL, it is not expected to obtain random copolymers in the copolymerization of these two monomers.[30] In accordance with the Mayo–Lewis equation, the composition of a copolymer can be expressed as a function of the initial monomer concentrations and reactivity ratios according to the terminal model, in which radical reactivity depends only on the identity of the terminal unit on the growing chain.[31] Following the Mayo–Lewis equation, the composition of the copolymers was calculated and it was determined that until a 20% of VCL in the feed, the mole fraction of VCL in the copolymer and the mole fraction of VCL in the feed were equal. In order to ensure the synthesis of random copolymers, the copolymerization reactions were carried out until 20% of conversion. Partial conversions of VCL and AA for both copolymers are shown in Fig. 1.

Conversion evolutions determined through ^{1}H-NMR show that the consumption rate of both monomers was similar in both cases, therefore it can be confirmed that short and long random copolymers were obtained.

Dibenzyl trithiocarbonate (DBTTC) is a symmetrical RAFT agent having two benzyl groups and therefore the polymeric chain can grow from both ends of this RAFT agent, obtaining in this way two benzyl end groups in the resulting copolymer. Assuming the presence of the residues of a single RAFT agent in each copolymer chain, the value of the theoretical number average molecular weight of the copolymer prepared ($M_{n,th}$) can be estimated by the following equation:

$$M_{n,th} = F_{AA} D_p M_{AA} + (1 - F_{AA}) D_P M_{VCL} + M_{RAFT}$$

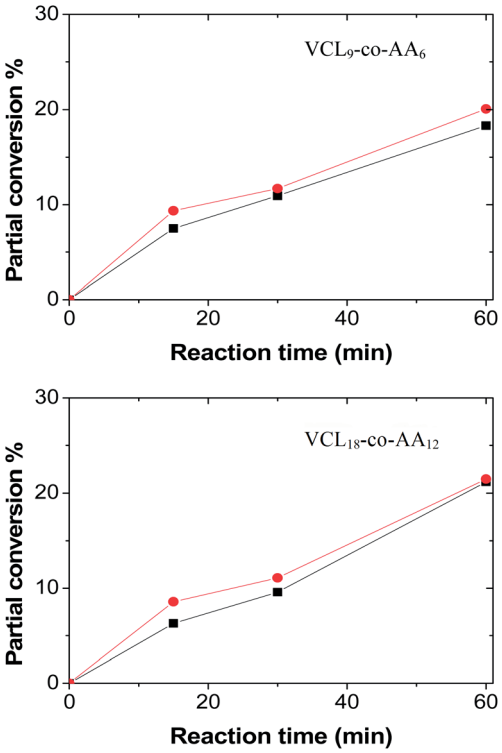

Fig. 1 Evolutions of the partial conversions of VCL (■) and AA (●) in the RAFT polymerizations of both anionic random copolymers.

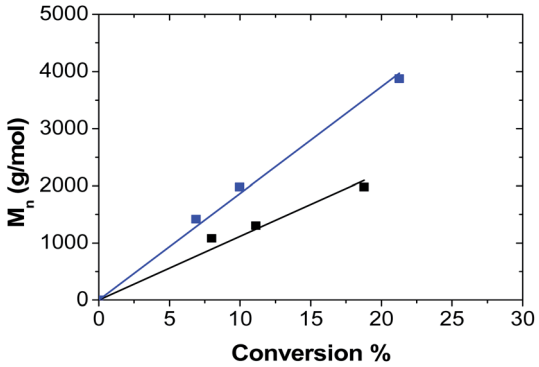

Fig. 2 M_n of the RAFT copolymers *versus* total conversion: ■ VCL_9-*co*-AA_6; ■ VCL_{18}-*co*-AA_{12}.

where F_{AA} is the mole fraction of AA in the copolymer, D_P is the number-average degree of polymerization and M_{AA}, M_{VCL} and M_{RAFT} are the molecular weights of AA, VCL and RAFT agent, respectively. The experimental value of M_n of random copolymers was measured by ^{1}H-NMR using end group analysis. In Table 1, theoretical ($M_{n,th}$) and experimental ($M_{n,NMR}$) average molecular weights are shown. As can be seen, experimentally determined M_n values correspond well with the theoretical ones for both, short (VCL_9-*co*-AA_6) and long (VCL_{18}-*co*-AA_{12}) copolymers.

In addition, in Fig. 2 the linear increase of M_n against conversion for both random copolymers is shown confirming that the synthesis of both copolymers was carried out under controlled conditions.

3.2 Adsorption studies

The complexation between a flexible polyelectrolyte and a charged surface of opposite sign is rather complex, depending on many parameters such as the charge and the size of the surface, the charge density on the polyion chain, the flexibility of the polyelectrolyte backbone, and the ionic strength of the medium.[32] Although the interaction between charged vesicles and polyelectrolytes is mainly electrostatic, their stronger adsorption is achieved, thanks to the hydrophobic interactions with the tails of the lipid molecules. In addition, the complexes are formed when the polyelectrolyte is amphiphilic, but do not bind in the absence of hydrophobic moieties on the polyelectrolyte chain. In order to increase the interaction between the cationic DODAB vesicles and the random copolymers synthesized (VCL_9-*co*-AA_6 and VCL_{18}-*co*-AA_{12}), the adsorption studies were performed at 55 °C (polyVCL (PVCL) hydrophobic, *i.e.* above its LCST), and at pH ~ 7 (polyAA (PAA) negatively charged). Mixtures of various compositions were studied under these conditions. The parameter used to express the composition of the mixtures is known as the stoichiometric charge ratio (ξ) and is defined as:[33]

$$\xi = \frac{N_{acid}[RAFT]}{[DODAB]}$$

where N_{acid} is the total number of acrylic acid units in the RAFT copolymer chain, and [RAFT] and [DODAB] are the molar concentrations of the RAFT copolymer and DODAB, respectively.

Fig. 3 shows the dependence of the normalized hydrodynamic diameter and polydispersity index (PDI) as a function of the charge ratio parameter (ξ).

As can be observed, the normalized hydrodynamic diameter was close to the diameter of the original DODAB vesicles until around a charge ratio parameter of 0.3 for both copolymers. The region between charge ratios from about 0.3 to 0.6 was marked by a sharp increase of the normalized hydrodynamic diameter and PDI. This increase suggests the formation of aggregates among partially covered vesicles. When the charge provided by the adsorbed polyelectrolyte coating is sufficient to neutralize the vesicle surface charge, the polyelectrolyte-coated vesicles have strong tendency to form aggregates. The reason behind this aggregation could be a non-homogeneous overcompensation of the surface charge of the cationic vesicles by the adsorbing RAFT anionic copolymers. The aggregates may be formed when one vesicle with a polyelectrolyte-covered domain interacts with another vesicle by binding to its non-covered

Table 1 Theoretical $M_{n,th}$, average copolymer compositions and experimental $M_{n,NMR}$

RAFT copolymer	$M_{n,th}$ (g mol^{-1})	NMR		VCL_x-*co*-AA_y		$M_{n,NMR}$ (g mol^{-1})
		D_P	F_{AA}	x	y	
VCL_9-*co*-AA_6	1992	15	0.4	9	6	1978
VCL_{18}-*co*-AA_{12}	3886	30	0.4	18	12	3875

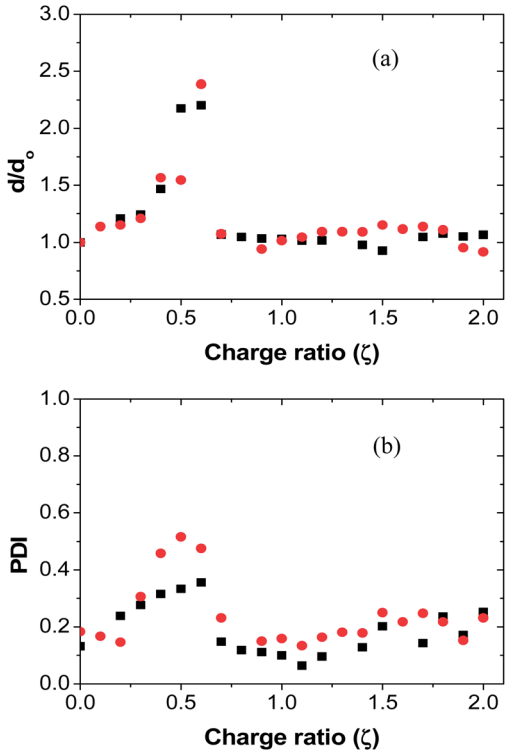

Fig. 3 Normalized hydrodynamic diameter (a) and polydispersity index (PDI) (b) as a function of the charge ratio (ξ): ■ VCL_9-*co*-AA_6; ● VCL_{18}-*co*-AA_{12}.

oppositely charge domain.[27] The closer the charge neutralization the bigger the average size of aggregates. Considering the same number of surfactant molecules in both layers of the DODAB vesicle bilayer,[27,28] the point of zero charge (isoelectric point) can be calculated following the charge ratio expression and it corresponds to a charge ratio value of around 0.5. As can be seen in Fig. 3, a maximum normalized hydrodynamic diameter value was obtained around 0.6 either for VCL_9-*co*-AA_6 and VCL_{18}-*co*-AA_{12} copolymers, close to the theoretical value. Increasing the amount of both RAFT anionic copolymers above a charge ratio of 0.7, the normalized hydrodynamic diameter and PDI decreased due to the formation of copolymer-covered anionically stabilized vesicles. In the case of both copolymers, VCL_9-*co*-AA_6 and VCL_{18}-*co*-AA_{12}, above a charge ratio of 0.7, sufficient amount of the anionic RAFT copolymer was absorbed onto the surface of the DODAB vesicles providing the required electrostatic repulsion. Therefore, in the synthesis of thermo-responsive nanocapsules, a charge ratio of 2 was used in order to avoid the formation of aggregates.

3.3 Thermal behavior of the nanocapsules

The chain length of the synthesized anionic RAFT copolymers could be an important factor for successful encapsulation of the DODAB vesicles. For an efficient encapsulation process, the RAFT copolymer should be small enough to give a maximum number of living moieties on the vesicle surface. However, RAFT copolymers that are too small and possess a smaller number of anchoring charge units are more prone to migrate into the aqueous phase and might cause problems on emulsion stability during the encapsulation reaction. In this work, two families of nanocapsules have been synthesized using the previously synthesized VCL_9-*co*-AA_6 and VCL_{18}-*co*-AA_{12} anionic RAFT copolymers.

At the first stage, thermo-sensitive nanocapsules were synthesized without using a cross-linker. Fig. 4 shows the effect of the length of the anionic RAFT copolymer on the temperature sensitivity of the final nanocapsule particles.

The sample was taken directly from the reactor and cooled while measuring the hydrodynamic diameter, and then a heating cycle was performed. As can be seen, in both cases, nanocapsules synthesized with VCL_9-*co*-AA_6 or VCL_{18}-*co*-AA_{12}, were shrunken above the LCST reducing their size due to an increase in the hydrophobic interactions between non-polar groups, and no hysteresis was observed between cooling and heating cycles. On the other hand, below the LCST, nanocapsule particles were swollen and hysteresis was observed between both cycles, the heating cycle showed an increase in the hydrodynamic diameter and polydispersity index. Below the LCST, intermolecular interactions between PVCL chains and water molecules *via* H-bonding increase dramatically, together with a weakening of the hydrophobic interactions inside the PVCL chains and therefore, PVCL chains tend to separate from DODAB vesicles leading to an increase in the hydrodynamic diameter and polydispersity indices (PDIs).[34]

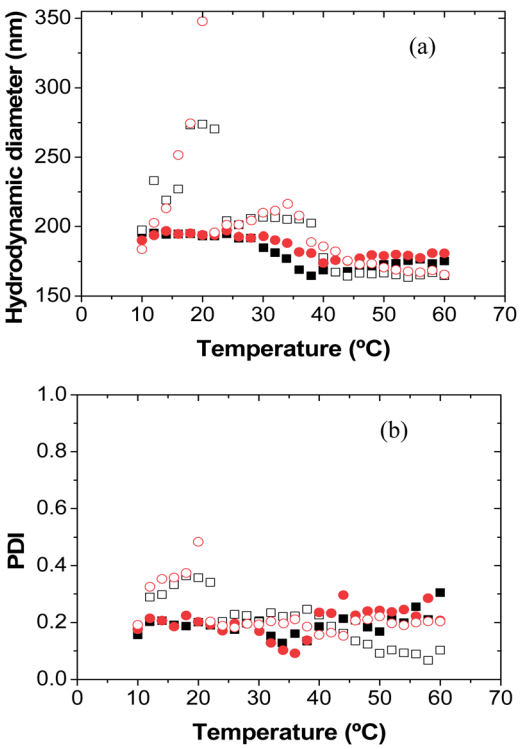

Fig. 4 Average hydrodynamic particle diameter (a) and polydispersity index (b) as a function of temperature for nanocapsules synthesized without cross-linker. ■ Cooling and □ heating cycle using VCL_9-*co*-AA_6 copolymer; ● cooling and ○ heating cycle using VCL_{18}-*co*-AA_{12} copolymer.

With the aim of avoiding the separation of PVCL chains from DODAB vesicles, thermo-sensitive nanocapsules were synthesized using MBA as the bifunctional cross-linker. In Fig. 5, the effect of the cross-linker amount on the thermal behavior of the final cross-linked nanocapsule particles synthesized using VCL_9-*co*-AA_6 and VCL_{18}-*co*-AA_{12} anionic RAFT copolymers is shown.

The results show that all the nanocapsule particles swell by a decrease in temperature and shrink at temperature above the VPTT. In addition, no hysteresis was observed between cooling and heating cycles at low temperatures, below the LCST of PVCL (32–38 °C). However, around the transition temperature hysteresis was observed between both cycles in the case of using either, VCL_9-*co*-AA_6 or VCL_{18}-*co*-AA_{12} copolymers. In Table 2, the VPTT values for cross-linked nanocapsules synthesized using both anionic copolymers and the differences in hydrodynamic diameters (Δdp) between cooling and heating cycles at the transition temperature are shown.

It is well known that the VPTT of PVCL-based nanogels can be modulated through incorporation of hydrophilic or hydrophobic comonomers in the polymerization recipe.[35,36] But, in this case the VPTT value was independent of the hydrophilicity/hydrophobicity of the cross-linkers used, at least in the studied range of the cross-linker concentration, as can be seen in Table 2. It seems that the type of interactions between PVCL chains and water molecules does not change in the presence of the cross-linker. Regarding the hysteresis between cooling and heating cycles around the transition temperature, as can be seen in Table 2, the differences in diameters between both cycles decreased as the cross-linker concentration increased. The same behavior was observed in the case of using either VCL_9-*co*-AA_6 or VCL_{18}-*co*-AA_{12} copolymers to synthesize thermo-responsive nanocapsules. This behavior can be explained due to the presence of PVCL homopolymer chains that are not cross-linked in the shell of the nanocapsules. When a low amount of cross-linker was used, because of the higher reactivity of the cross-linker compared to that of the main monomer (VCL), nanocapsules consisted of a large shell mainly containing non-cross-linked VCL units were formed. Increasing the amount of cross-linker, although non-cross-linked PVCL chains also formed the shell, these chains were more entangled. Therefore, the PVCL chain movement was restricted decreasing the hysteresis between cooling and heating cycles.

Table 2 VPTTs and Δdp for the nanocapsules synthesized using MBA or EGDMA as cross-linkers

RAFT copolymer	Amount of MBA	VPTT (°C)	Δdp[a] (nm)
VCL_9-*co*-AA_6	4 mol%	33.7	34
	8 mol%	33.2	28
	12 mol%	33.2	26
VCL_{18}-*co*-AA_{12}	4 mol%	35.8	27
	8 mol%	34.2	24
	12 mol%	34.8	19
RAFT copolymer	Amount of EGDMA	VPTT (°C)	Δdp[a] (nm)
VCL_9-*co*-AA_6	4 mol%	33.6	20
	8 mol%	33.2	20

[a] $\Delta dp = (dp_{heating} - dp_{cooling})$.

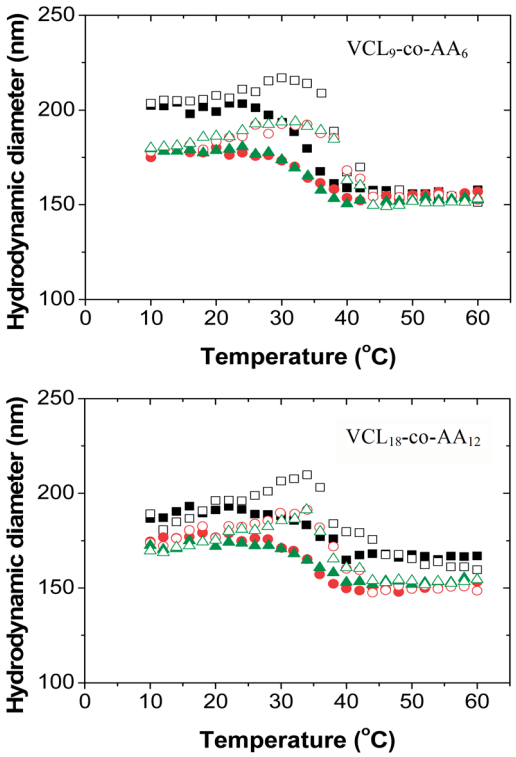

Fig. 5 Average hydrodynamic particle diameter as a function of temperature for nanocapsules synthesized using different amounts of MBA as the cross-linker. ■ Cooling and □ heating cycle using 4 mol%. ● Cooling and ○ heating cycle using 8 mol%. ▲ Cooling and △ heating cycle using 12 mol%.

For the sake of comparison, thermo-sensitive nanocapsules were synthesized using VCL_9-*co*-AA_6 as the anionic RAFT copolymer and EGDMA as the cross-linker. In Fig. 6, the effect of the amount of EGDMA used on the thermal behavior of the final nanocapsules is shown.

The results show that all final nanocapsules were swollen by decreasing the temperature of the medium in which they were dispersed and they were collapsed at temperatures above the VPTT, as expected. As can be seen in Table 2, in the case of nanocapsules synthesized using MBA as the cross-linker, the VPTT was independent of the EGDMA concentration. In addition, as can be observed in Fig. 6, nanocapsules synthesized using EGDMA as the cross-linker also presented hysteresis around the transition temperature.

Regarding the hysteresis presented around the VPTT, in the case of using EGDMA as the cross-linker, the difference between the cooling and heating cycle was less than in the case of using the same amount of MBA, as can be seen in Table 2. At this point, it is important to take into account the availability of the cross-linker in the reaction mixture. Imaz and Forcada reported that during emulsion polymerization of VCL using poly(ethylene

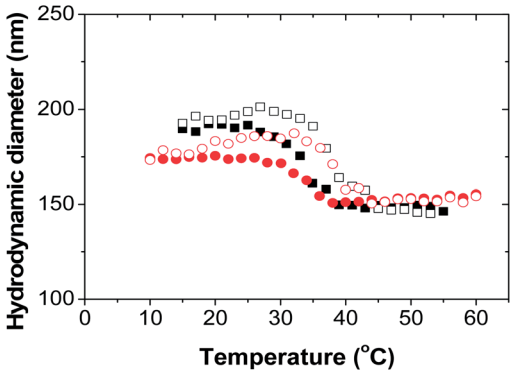

Fig. 6 Average hydrodynamic particle diameter as a function of temperature for nanocapsules synthesized using different amounts of EGDMA as cross-linker and VCL_9-*co*-AA_6 copolymer. ■ Cooling and □ heating cycle using 4 mol%. ● Cooling and ○ heating cycle using 8 mol%.

glycol) diacrylate (PEGDA) or MBA as cross-linkers, both cross-linkers were consumed faster compared to VCL.[37] The same behavior could be considered in the case of using EGDMA and MBA as cross-linkers, suggesting that MBA reacted faster than EGDMA due to the higher water solubility of MBA (19.4 mmol L^{-1}) compared to that of EGDMA (5.4 mmol L^{-1}) and because of the fact that polymerization took place in the water phase. Therefore, the distribution of EGDMA was more homogeneous through nanocapsules and the PVCL chain movement was more restricted than in the case of using the same amount of MBA, decreasing the hysteresis around the VPTT between cooling and heating cycles.

Fig. 7 shows the effect of the type of cross-linker on the swelling ratio of the final nanocapsules.

In the case of using either MBA or EGDMA, increasing the amount of cross-linker from 4 mol% to 8 mol%, the swelling ratio decreased as expected due to the increase in the degree of cross-linking of the final nanocapsule particles. On the other hand, when the same amounts of MBA and EGDMA were used, as both cross-linkers are bifunctional the same swelling ratio as a function of temperature was obtained due to the same amount of reactive groups used which is capable of cross-linking of PVCL.

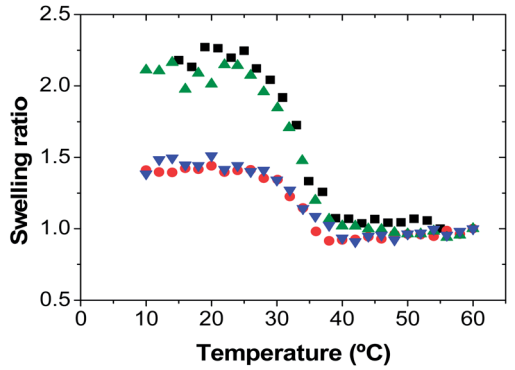

Fig. 7 Effect of the type of cross-linker on the swelling ratio as a function of temperature for nanocapsules synthesized using VCL_9-*co*-AA_6 anionic RAFT copolymer. ■ 4 mol% of EGDMA; ● 8 mol% of EGDMA; ▲ 4 mol% of MBA; ▼ 8 mol% of MBA.

TEM was used to examine the morphology of the resulting thermo-sensitive nanocapsules. Fig. 8 shows the nanocapsules obtained by templating DODAB vesicles using VCL_9-*co*-AA_6 and VCL_{18}-*co*-AA_{12} anionic RAFT copolymers and MBA and EGDMA cross-linkers. As can be observed, in all the cases hollow nanocapsules were obtained. The diameters measured by PCS were smaller than those analyzed by TEM due to the drying process; during drying nanocapsules could be crushed and distorted increasing their size. Ali *et al.*[29] observed that long RAFT copolymers, due to their limited solubility, could possibly collapse in the form of very small particles and induce the formation of free polymer particles in the aqueous phase. However, as can be seen in Fig. 8, secondary nucleations were not observed, even in the case of using the longer anionic RAFT copolymer (VCL_{18}-*co*-AA_{12}). In addition, increasing the amount of cross-linker (MBA or EGDMA) more spherical and consistent nanocapsules were obtained (see Fig. 8c, f and h).

To study in depth the formation of the polymeric shell around DODAB vesicles, the gel-to-liquid crystalline transition temperature (T_m) of the thermo-responsive nanocapsules was determined. The gel-to-liquid crystalline phase transition is an important intrinsic property of the vesicle bilayer since T_m indicates its stability and permeability. Below this transition temperature, the amphiphilic DODAB molecules form lamellar crystalline phases and above the transition temperature, because of the increase of thermal motions, these molecules are less tightly packed. Therefore, the bilayer thickness decreases and its permeability increases.[38] The presence of a polymeric shell around a DODAB vesicle results in increase of T_m due to the protection that the polymer confers on the vesicle bilayer. To evaluate the formation of the polymeric shell, the absorbance dependence on temperature of the thermo-sensitive nanocapsules was determined. Table 3 summarizes the values of T_m for thermo-sensitive nanocapsules synthesized varying the length of the RAFT copolymers synthesized and the type and amount of cross-linker.

The T_m value determined for naked DODAB vesicles was 37.5 °C, and as can be seen in Table 3, in all the cases the T_m values for the thermo-sensitive nanocapsules were higher, which means that in all the cases onto DODAB vesicles a polymeric shell was obtained. It is interesting to point out that non-crosslinked nanocapsules also showed a higher transition temperature, as can be seen in Table 3. In the case of the cross-linked nanocapsule particles, as the amount of cross-linker increased the T_m values decreased. The decrease in T_m for cross-linked nanocapsules can be explained on the basis of the vesicle curvature.[38] In the case of more curved vesicles, the melting process is more favored due to a less efficient packing of DODAB molecules. Therefore, when increasing the amount of cross-linker more spherical and consistent nanocapsules were obtained, as was confirmed by TEM images, and the T_m values determined were lower.

3.4 Stability of the nanocapsules

Thanks to their hollow structure, nanocapsules are potentially useful for encapsulation of various chemical molecules, being

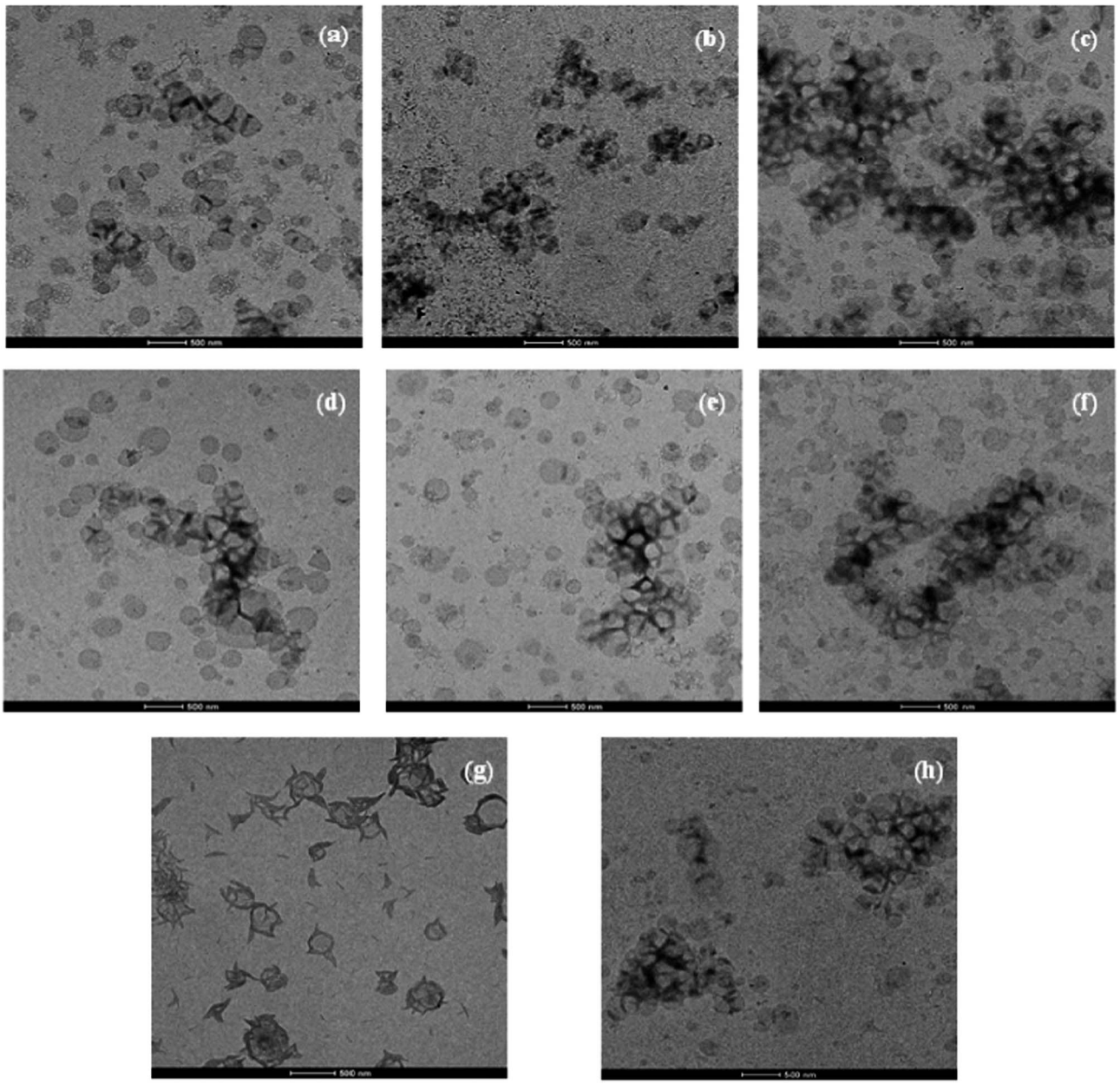

Fig. 8 TEM microphotographs of the final nanocapsules VCL_9-*co*-AA_6 copolymer and MBA: (a) 4 mol%, (b) 8 mol%, and (c) 12 mol%; VCL_{18}-*co*-AA_{12} copolymer and MBA: (d) 4 mol%, (e) 8 mol%, and (f) 12 mol%; and VCL_9-*co*-AA_6 copolymer and EGDMA: (g) 4 mol%, and (h) 8 mol%.

suitable for drug delivery. In order to use them as drug carriers and avoid early delivery of the encapsulated drugs, these nanocapsules must be stable. However, it is known that the addition of a monotailed surfactant to vesicle dispersion can destabilize the vesicles, leading to their complete breakdown into mixed micelles. This happens due to the incorporation of surfactant molecules into the vesicle bilayer until the concentration of the surfactant reaches a critical value. After that critical value, the vesicles start breaking up into bilayer fragments which eventually transform into mixed micelles. Thanks to the protection of the polymeric shell and therefore having higher stability, nanocapsules are more attractive for drug delivery than surfactant vesicles.[39] However, it is important to understand how amphiphilic molecules, especially those occurring naturally in the body, can interact with nanocapsules and check their possible disruption due to the presence of those amphiphilic molecules.

The formation of stable polymeric nanocapsules can be confirmed by surfactant lysis experiments. In this work, the non-anionic surfactant Triton X-100 was used due to its properties as a good solubilization agent for membrane proteins.[40] In order to probe the stability of the thermo-sensitive nanocapsules synthesized, optical density and dynamic light scattering measurements were carried out.

In Fig. 9, the optical density as a function of molar ratio of Triton X-100 and DODAB at 50 °C is shown.

At this point, it is important to take into account that at 50 °C, the thermo-sensitive nanocapsules were collapsed

Table 3 T_m values for the nanocapsules synthesized using both anionic RAFT copolymers and MBA or EGDMA cross-linkers

	Cross-linker		
Anionic RAFT copolymer	Type	Amount	T_m (°C)
VCL_9-*co*-AA_6	MBA	0 mol%	45
		4 mol%	45
		8 mol%	47.5
		12 mol%	42.5
	EGDMA	4 mol	45
		8 mol%	45
VCL_{18}-*co*-AA_{12}	MBA	0 mol%	47.5
		4 mol%	47.5
		8 mol%	45
		12 mol%	42.5

because the temperature was above the VPTT. As can be seen, naked DODAB vesicles presented a typical three-stage disintegration profile.[27] At low Triton X-100 concentration, below the molar ratio of [Triton X-100]/[DODAB] of 0.8, an initial increase of the normalized optical intensity was observed due to the incorporation of surfactant molecules into the bilayer and the maximum value was reached for bilayer saturation. Increasing amounts of surfactant led to a fall in the scattered intensity until a low constant value, in which mixed micelles were formed. However, in the case of thermo-sensitive nanocapsules, the typical three-stage transition from vesicles to micelles was not observed. In all the cases, either using short or long anionic copolymers and with or without cross-linkers, a decrease in the normalized optical density was observed after every injection of surfactant, but this decrease was only due to a dilution effect and breakdown of some non-covered DODAB vesicles that might be in the dispersion. The same behavior was observed when the amount of cross-linker was increased from 4 mol% to 8 and 12 mol% (data not shown).

In order to study in depth the stability of the thermo-sensitive nanocapsules, dynamic light scattering measurements were carried out at 50 °C (see Fig. S1 in the ESI†). Before mixing with Triton X-100, the size distribution of DODAB vesicles was monomodal, averaging around a diameter of about 160 nm. After mixing with Triton X-100 at a molar ratio of [Triton X-100]/[DODAB] of 3, different peaks appeared in the distribution below 100 nm due to the formation of DODAB–Triton X-100 mixed micelles.

On the other hand, in the case of mixing Triton X-100 with thermo-sensitive nanocapsules, although new peaks appeared below 100 nm, the nanocapsules' average diameters remained around their initial size. It is interesting to point out that non-crosslinked nanocapsules were also stable to surfactant lysis experiments at 50 °C (collapsed state). It is important to take into account that these experiments were carried out at 50 °C and therefore, PVCL-based nanocapsules were in their collapsed state. For this reason, it was supposed that nanocapsules were more consistent being more difficult their disruption. The appearance of peaks below 100 nm is another piece of evidence of the existence of non-covered DODAB vesicles in the dispersion. The same behavior was observed when the amount of cross-linker was increased from 4 mol% to 8 and 12 mol% (data not shown).

Apart from studying the stability at high temperature, PVCL-based nanocapsules being collapsed, the same measurements were carried out at 20 °C for the nanocapsules synthesized using the VCL_9-*co*-AA_6 copolymer and MBA as the cross-linker. Below the VPTT, nanocapsules were highly swollen, their structure being looser and less compact than those above the VPTT. Therefore they could be more vulnerable to the incorporation of Triton X-100 molecules, the disruption of the nanocapsules being easier in this way. As can be seen in Fig. 10a, the normalized optical density decreased after every injection of surfactant.

As discussed before, the decrease in normalized optical density was only due to a dilution effect and breakdown of some non-covered DODAB vesicles that might be in the dispersions. On the other hand, as can be seen in Fig. 10b, after mixing Triton X-100 and the nanocapsule dispersion at 20 °C, the nanocapsule average diameter remained around its initial size. In this case also, a new peak appeared around 10 nm due to the disruption of non-covered DODAB vesicles.

It is remarkable that the stability of the synthesized thermo-responsive nanocapsules was confirmed at low and high temperatures, demonstrating thqe potential use of these nanocapsules as drug delivery carriers.

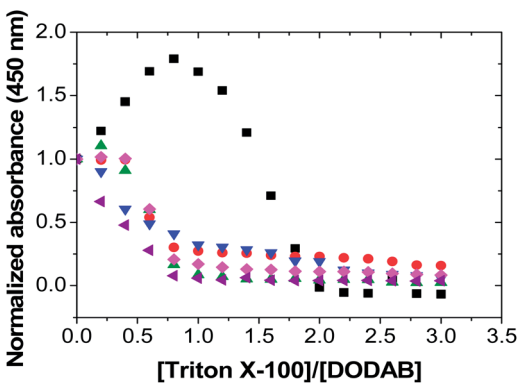

Fig. 9 Normalized optical density as a function of Triton X-100/DODAB molar ratio: ■ DODAB vesicles; family of VCL_9-*co*-AA_6 copolymer ● without cross-linker; ▲ 4 mol% of MBA; ▼ 4 mol% of EGDMA; family of VCL_{18}-*co*-AA_{12} copolymer ◆ without cross-linker; and ◀ 4 mol% of MBA.

4. Conclusions

The synthesis of thermo-responsive and biocompatible cross-linked nanocapsules through dimethyldioctadecylammonium bromide (DODAB) vesicle templating was reported for the first time. Prior to the synthesis of the nanocapsules, two random copolymers of VCL and AA with different chain lengths were synthesized by RAFT polymerization and adsorbed onto previously prepared DODAB vesicles. After adsorbing the random anionic copolymers, thermo-responsive hollow nanocapsules were synthesized by semicontinuous emulsion polymerization under monomer-starved conditions for both the main

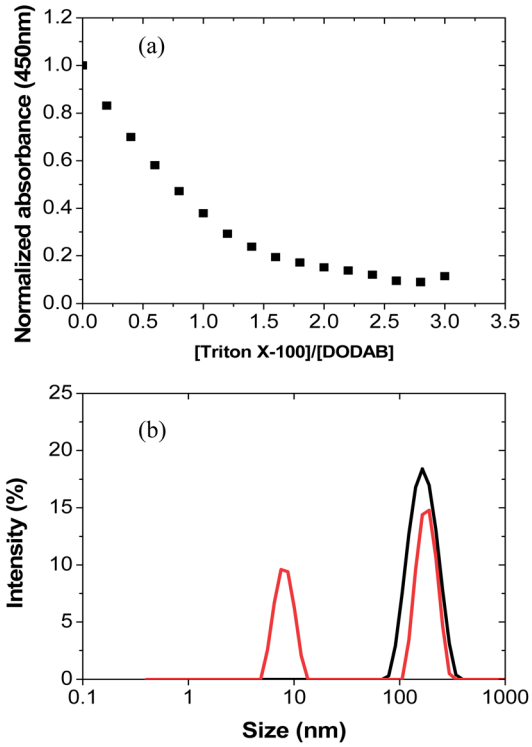

Fig. 10 Normalized optical density as a function of [Triton X-100]/[DODAB] (a) and particle size distributions before (black line) and after (red line) Triton X-100 addition (b) of the nanocapsules synthesized using VCL_9-*co*-AA_6 copolymer and 4 mol% of MBA, at 20 °C.

monomer (VCL) and the cross-linker (MBA or EGDMA). The colloidal characteristics, taking into account the length of the copolymers and the cross-linker concentration and type, were studied by analyzing average diameters together with the swelling behavior and gel-to-crystalline phase transition temperature of the nanocapsules synthesized.

The results showed that the non-cross-linked nanocapsules present hysteresis at low temperatures between cooling and heating cycles due to the tendency of PVCL chains to separate from DODAB vesicles either in the case of using short or long random anionic copolymers. On the other hand, using both VCL_9-*co*-AA_6 or VCL_{18}-*co*-AA_{12} copolymers, and MBA as the cross-linker, the hysteresis disappeared at low temperature, but not around the VPTT. Increasing the amount of MBA both, the hysteresis between both cycles and the swelling ratio decreased due to the restriction or hindrance of the PVCL chain movement. In addition, the formation of more spherical and consistent nanocapsules was observed by TEM, increasing the amount of cross-linker either using VCL_9-*co*-AA_6 or VCL_{18}-*co*-AA_{12} random copolymer. Furthermore, due to the increase in curvature, lower values of T_m were obtained when increasing the amount of cross-linker. In the case of using EGDMA as the cross-linker, the observed hysteresis around the VPTT was less due to the more homogeneous distribution of EGDMA into the nanocapsules. The amount of EGDMA had the same effect as MBA on the swelling capacity and T_m values.

Since the stability of the nanocapsules is a compulsory requirement if they are used as nanocarriers, surfactant lysis experiments were carried out in order to ensure their stability at low and high temperatures. The results showed that nanocapsules were stable regardless of using short or long anionic copolymers and MBA or EGDMA as cross-linkers. Moreover, their stability below (swollen state) and above (collapsed state) the VPTT was confirmed.

Thanks to their hollow morphology, biocompatibility and capacity of undergoing reversible volume phase transitions in response to temperature, the nanocapsules synthesized can be considered as promising nanocarriers in controlled drug delivery. In addition, the use of vesicles as soft templates enhances the suitability of the nanocapsules synthesized as nanocarriers, allowing the pre-encapsulation of different drugs before their formation.

Acknowledgements

This work has been supported by the Spanish Plan Nacional de Materiales (MAT2012-36,270-C04-01) and UFI 11/56 of the University of the Basque Country UPV/EHU. G. Aguirre thanks Mohammad Amin Moradi for his valuable help in the preparation of DODAB vesicles. Technical support provided by SGIker (UPV/EHU, MICINN, GV/EJ, ESF) is gratefully acknowledged.

References

1 J. Ramos, J. Forcada and R. Hidalgo-Alvarez, *Chem. Rev.*, 2014, **114**, 367.
2 C. E. Mora-Huertas, H. Fessi and A. Elaissari, *Int. J. Pharm.*, 2010, **385**, 113.
3 W. Yajun, V. Bansal, A. N. Zelikin and F. Caruso, *Nano Lett.*, 2008, **8**, 1741.
4 S. M. Marinakos, J. P. Novak, L. C. Brousseau III, A. B. House, E. H. Edeki, C. Feldhaus and D. L. Feldheim, *J. Am. Chem. Soc.*, 1999, **121**, 8518.
5 F. T. Liu and A. Eisenberg, *J. Am. Chem. Soc.*, 2003, **125**, 15059.
6 Y. W. Zhang, M. Jiang, J. X. Zhao, Z. X. Wang, H. J. Dou and H. J. Chen, *Langmuir*, 2005, **21**, 1531.
7 B. Mu, P. Liu, Z. Tang, P. Du and Y. Dong, *Nanomedicine*, 2011, **7**, 789.
8 G. Ibarz, L. Dahne, E. Donath and H. Mohwald, *Adv. Mater.*, 2001, **13**, 1324.
9 N. Singh and A. Lyon, *Chem. Mater.*, 2007, **19**, 719.
10 J. Qian and F. P. Wu, *Chem. Mater.*, 2007, **19**, 5839.
11 H. Wei, D. Q. Wu, Q. Li, C. Chang, J. P. Zhou, X. Z. Zhang and R. X. Zhuo, *J. Phys. Chem. C*, 2008, **112**, 15329.
12 A. Imaz and J. Forcada, *J. Polym. Sci., Part A: Polym. Chem.*, 2010, **48**, 1173.
13 A. C. W. Lau and C. Wu, *Macromolecules*, 1999, **32**, 581.
14 J. Ramos, A. Imaz and J. Forcada, *Polym. Chem.*, 2012, **3**, 852.
15 B. C. Lokitz, A. York, W. J. E. Stempka, N. D. Treat, Y. Li, W. L. Jarret and C. L. McCormick, *Macromolecules*, 2007, **40**, 6473.

16 S. Wang, M. Jiang and G. Z. Zhang, *Macromolecules*, 2007, **40**, 5552.
17 F. Chécot, J. Rodríguez-Hernández, Y. Gnanou and S. Lecommandoux, *Polym. Adv. Technol.*, 2006, **17**, 782.
18 E. Donath, G. B. Sukhorukov, F. Caruso, S. A. Davis and H. Möhwald, *Angew. Chem., Int. Ed.*, 1998, **37**, 2201.
19 A. P. R. Johnston, C. Cortez, A. S. Angelatos and F. Caruso, *Curr. Opin. Colloid Interface Sci.*, 2006, **11**, 203.
20 Y. Fukui and K. Fujimoto, *Langmuir*, 2009, **25**, 10020.
21 M. Germain, S. Grube, V. Carriere, H. Richard-Foy, M. Winterhalter and D. Fournier, *Adv. Mater.*, 2006, **18**, 203.
22 I. Pastoriza-Santos, B. Schöler and F. Caruso, *Adv. Funct. Mater.*, 2001, **11**, 122.
23 M. Kepczynski, J. Lewandowska, M. Romek, S. Zapotoczny, F. Ganachaud and M. Nowakowska, *Langmuir*, 2007, **23**, 7314.
24 J. Hotz and W. Meier, *Langmuir*, 1998, **14**, 1031.
25 M. Germain, G. Stephan, V. Carriere, H. Richard-Foy, M. Winterhalter and D. Fournier, *Adv. Mater.*, 2006, **18**, 2868.
26 F. Cuomo, F. Lopez, M. G. Miguel and B. Lindman, *Langmuir*, 2010, **26**, 10555.
27 S. I. Ali, J. P. A. Heuts and A. M. van Herk, *Langmuir*, 2010, **26**, 7848.
28 S. I. Ali, J. P. A. Heuts and A. M. van Herk, *Soft Matter*, 2011, **7**, 5382.
29 S. I. Ali, J. P. A. Heuts, B. S. Hawkett and A. M. van Herk, *Langmuir*, 2009, **25**, 10523.
30 J. I. Brandrup, H. Edmund, E. Grulke, A. Abe and D. R. Bloch, *Polymer Handbook*, Wiley-Interscience, New York, 4th edn, 2005, vol. I, p. 247.
31 F. R. Mayo and F. M. Lewis, *J. Am. Chem. Soc.*, 1944, **66**, 1594.
32 F. Bordi, C. Cametti, M. Diociaiuti, D. Gaudino, T. Gili and S. Sennato, *Langmuir*, 2004, **20**, 5214.
33 D. Volodkin, H. Mohwald, J. C. Volgel and V. J. Ball, *J. Controlled Release*, 2007, **117**, 111.
34 F. Meeussen, E. Nies, H. Berghmans, S. Verbrugghe, E. Goethals and F. Du Prez, *Polymer*, 2000, **41**, 8597.
35 A. Imaz and J. Forcada, *Eur. Polym. J.*, 2009, **45**, 3164.
36 A. Imaz and J. Forcada, *J. Polym. Sci., Part A: Polym. Chem.*, 2011, **49**, 3218.
37 A. Imaz and J. Forcada, *J. Polym. Sci., Part A: Polym. Chem.*, 2008, **46**, 2766.
38 E. Feitosa, P. C. A. Barreleiro and G. Olfsson, *Chem. Phys. Lipids*, 2000, **105**, 201–213.
39 M. Kepczynski, J. Lewandowska, M. Romek, S. Zapotoczny, F. Ganachaud and M. Nowakowska, *Langmuir*, 2010, **23**, 7314.
40 A. De La Maza and J. L. Parra, *Biochem. J.*, 1994, **303**, 907.